FBW7 mutations in leukemic cells mediate NOTCH pathway activation and resistance to γ-secretase inhibitors

Jennifer O'Neil,[1] Jonathan Grim,[2] Peter Strack,[3] Sudhir Rao,[3] Deanne Tibbitts,[4] Christopher Winter,[3] James Hardwick,[5] Markus Welcker,[2] Jules P. Meijerink,[6] Rob Pieters,[6] Giulio Draetta,[3] Rosalie Sears,[4] Bruce E. Clurman,[2] and A. Thomas Look[1,7]

[1]Department of Pediatric Oncology, Dana-Farber Cancer Institute, Boston, MA 02115
[2]Division of Human Biology, Fred Hutchinson Cancer Research Center, Seattle, WA 98109
[3]Merck Research Laboratories, Boston, MA 02115
[4]Department of Molecular and Medical Genetics, Oregon Health and Sciences University, Portland, OR 97239
[5]Merck Research Laboratories, West Point, PA 19486
[6]Department of Pediatric Oncology/Hematology, Erasmus MC/Sophia Children's Hospital, 3000 CB Rotterdam, Netherlands
[7]Division of Hematology, Children's Hospital Boston, Boston, MA 02115

γ-secretase inhibitors (GSIs) can block NOTCH receptor signaling in vitro and therefore offer an attractive targeted therapy for tumors dependent on deregulated NOTCH activity. To clarify the basis for GSI resistance in T cell acute lymphoblastic leukemia (T-ALL), we studied T-ALL cell lines with constitutive expression of the NOTCH intracellular domain (NICD), but that lacked C-terminal truncating mutations in *NOTCH1*. Each of the seven cell lines examined and 7 of 81 (8.6%) primary T-ALL samples harbored either a mutation or homozygous deletion of the gene *FBW7*, a ubiquitin ligase implicated in NICD turnover. Indeed, we show that FBW7 mutants cannot bind to the NICD and define the phosphodegron region of the NICD required for FBW7 binding. Although the mutant forms of FBW7 were still able to bind to MYC, they do not target it for degradation, suggesting that stabilization of both NICD and its principle downstream target, MYC, may contribute to transformation in leukemias with *FBW7* mutations. In addition, we show that all seven leukemic cell lines with *FBW7* mutations were resistant to the MRK-003 GSI. Most of these resistant lines also failed to down-regulate the mRNA levels of the NOTCH targets *MYC* and *DELTEX1* after treatment with MRK-003, implying that residual NOTCH signaling in T-ALLs with *FBW7* mutations contributes to GSI resistance.

CORRESPONDENCE
A. Thomas Look:
Thomas_Look@dfci.harvard.edu
OR
Bruce E. Clurman:
bclurman@fhcrc.org

Abbreviations used: AML, acute myeloid leukemia; CPD, Cdc phosphodegron; GSI, γ-secretase inhibitor; MDS, myelodysplastic syndrome; NICD, NOTCH intracellular domain; T-ALL, T cell acute lymphoblastic leukemia.

The mammalian NOTCH proteins are heterodimeric transmembrane receptors that control cell proliferation, apoptosis, and cell fate during the development of diverse cellular lineages (1). Aberrant NOTCH signaling has been extensively linked to cancer and development. In mouse models, constitutive NOTCH signaling contributes to the genesis of breast cancer, medulloblastoma, and T cell leukemia (2–9), whereas in human cancer its role is best exemplified by T cell acute lymphoblastic leukemias (T-ALLs). Human *NOTCH1* was first discovered as a gene activated at the breakpoint of the t(7;9), a very rare chromosomal translocation that fuses the intracellular form of NOTCH1 to the T cell receptor β locus in lymphoblasts of T-ALL patients (10). Recently, 50% of human T-ALL cell lines and primary patient samples were shown to harbor activating mutations in *NOTCH1* that result in aberrant NOTCH signaling (11). Although mutations that directly activate NOTCH receptors have not been identified in other types of human cancers, there is abundant evidence to support the importance of deregulated NOTCH activity in the development of ovarian cancer (12), breast cancer (13), anaplastic large cell lymphoma and Hodgkin disease (14), melanoma (15), gliomas (16), lung carcinomas (17, 18), and cancers of the pancreas (18) and prostate (19). Hence, modulation of the NOTCH signaling cascade

J. O'Neil and J. Grim, and B.E. Clurman and A.T. Look contributed equally to this work.

at one or more points could short-circuit this pathway in NOTCH-supported tumors, leading to clinically important antitumor effects.

Blocking the intramembranous cleavage of NOTCH is an especially attractive strategy of targeted therapy. When the NOTCH receptor is recognized by its membrane-bound ligand, a conformational change exposes the receptor to sequential rounds of protease cleavage. Binding of the ligand results in proteolytic cleavage of the receptor, first outside the cell by TNF-α–converting enzyme and then by the γ-secretase membrane protease complex, releasing the NOTCH intracellular domain (NICD), which translocates to the nucleus where it regulates the expression of its target genes, including *MYC* and *DELTEX1* (20–23). Small molecule inhibitors of γ-secretase activity are now available that effectively inhibit NOTCH signaling in vitro. One commercial product, compound E, induces growth arrest in several different T-ALL cell lines by inhibiting the NOTCH pathway (11). Recently, we showed that treatment of T-ALL cells with the MRK-003 γ-secretase inhibitor (GSI) results in prolonged cell cycle arrest followed by apoptosis (24).

Despite the promise of GSI therapy for tumors driven by aberrant NOTCH signaling, most human T-ALL cell lines are resistant to these agents and grow normally despite GSI treatment. Thus, to establish the molecular basis of GSI resistance in tumor cells, we used T-ALL cell lines as a model system to test the ability of GSI treatment to reduce cellular levels of NICD, as well as its transcriptional targets *MYC* and *DELTEX1*. We found that mutations affecting the FBW7 ubiquitin ligase occur in GSI-resistant cell lines and are associated with sustained NOTCH signaling. Moreover, we found *FBW7* mutations in primary T-ALL samples, and the mutational spectrum suggests that they produce dominant-negative *FBW7* alleles. Our findings implicate *FBW7* mutations in both the pathogenesis of T-ALL and leukemic cell resistance to GSIs.

RESULTS

MRK-003 treatment leads to Notch-dependent antiproliferative effects in a subset of T-ALL cell lines

To inhibit NOTCH-mediated signal transduction, we treated each of 20 T-ALL cell lines with the Merck GSI MRK-003 (24) at 1 μM or with DMSO (vehicle control) for 7 d. To study the effects of GSI treatment, we analyzed the cell counts, cell cycle profiles, and apoptosis at various time points after treatment. We did not observe any effects on proliferation or viability at 6 h, 24 h, or 3 d in any of the 20 lines. Five of the T-ALL cell lines (DND41, Koptk1, ALL-SIL, HPB-ALL, and TALL1) were sensitive to GSI treatment, exhibiting two- to threefold fewer live cells in the GSI-treated flasks compared with DMSO-treated flasks on day 7 of treatment (Table I). Cell cycle analysis at that time revealed a G_0/G_1 cell cycle arrest with decreased cells in the S phase in each of the five lines (representative histograms are shown for one line in Fig. 1 A). Annexin V staining showed a two- to fourfold increase in the percentage of cells undergoing apoptosis in the five GSI-sensitive cell lines, indicating that MRK-003 acts by inducing apoptosis as well as by blocking cell growth (Fig. 1 B). Importantly, the altered proliferation, cell cycle arrest, and increase in apoptosis could be rescued by overexpressing the NICD, demonstrating that these effects indeed result from inhibition of the NOTCH signaling pathway (24 and unpublished data). The cell counts, cell cycle profiles, and percentages of apoptotic cells in the remaining 15 T-ALL cell lines were not affected by treatment with MRK-003 (Fig. 1, C and D, and Table I).

NICD levels are high in several T-ALL cell lines without truncating mutations in *NOTCH1*

Treatment with MRK-003 led to reduced levels of NICD in each of the T-ALL cell lines in which the intracellular protein could be detected, indicating that the compound effectively inhibited NOTCH1 cleavage at the cell surface (Fig. 1 E). However, only a subset of the 20 T-ALL cell lines had a GSI-sensitive cellular phenotype, indicating that a resistant phenotype can be observed with or without evidence for constitutive NOTCH signaling (i.e., without detectable expression of NICD; Table I and Fig. 1 E). Western blot analysis also demonstrated that all of the cell lines with C-terminal truncating mutations of *NOTCH1* expressed high levels of NICD (Table I and Fig. 1 E), reflecting aberrant activation of the NOTCH pathway. Interestingly, there were seven cell lines without C-terminal truncating mutations in *NOTCH1* that also expressed high levels of NICD (RPMI8402, CEM, BE13, DU528, HSB2, Jurkat, and PEER), implying that NOTCH is stabilized in these cell lines through a mechanism other than mutation of *NOTCH1*.

FBW7 is mutated in T-ALL cell lines and primary samples

Cellular levels of NICD are determined by the net effects of the rates of production and destruction of the protein. The SCF-FBW7 ubiquitin ligase plays a critical role in NICD degradation that is dependent on an intact PEST domain of NOTCH (25–30). Other known FBW7 substrates include cyclin E, MYC, SR-EBP, and c-Jun (31). FBW7 interacts with its substrates via the β propeller formed by its WD40 repeats after the substrate becomes phosphorylated within highly conserved Cdc phosphodegrons (CPDs) (32, 33). Human tumors harbor nonsense mutations that truncate FBW7 as well as missense mutations that target key arginine residues in the WD40 repeats. These mutations disable FBW7–substrate interactions and impair substrate degradation by FBW7 (34–37). Mutations affecting CPDs in tumor-derived alleles of both *MYC* and *JUN* have been described (38–41). Thus, mutations removing or altering the substrate CPD can also lead to loss of regulation by FBW7. Because the PEST domain truncations found in human T-ALL are predicted to disrupt FBW7 binding to NICD, we hypothesized that *FBW7* mutation could represent an alternative mechanism for NOTCH deregulation in human cancers.

To test this hypothesis, we sequenced the entire coding region of *FBW7* to determine whether mutations affecting

Table I. *FBW7* mutations in human T-ALL cell lines

	NOTCH1 status[a]			
	HD domain	PEST domain	NICD detected[b]	*FBW7* status
Sensitive Cell Lines				
DND41	heterozygous mutation 1594 L→P	heterozygous insertion 2444 CCSHWAPAAWRCTLFCPRRAPPCP RRCHPRWSHP*STOP	Yes	WT
HPB-ALL	heterozygous mutation 1575 L→P	heterozygous insertion 2442 EGRGRCSHWAPAAWRCTLFCPRRAPPCPRRCHPRWSHP*STOP	Yes	WT
Koptk1	heterozygous mutation 1601 L→P	heterozygous deletion 2515 RVP*STOP	Yes	WT
ALL-SIL	heterozygous mutation 1594 L→P	heterozygous insertion 2476 AHP*STOP	Yes	WT
TALL1	WT	WT	No	WT
Resistant Cell Lines				
RPMI8402	heterozygous insertion 1584 PVELMPPE	WT	Yes	homozygous mutation 465 R→H
CEM	heterozygous insertion 1595 PRLPHNSSFHFL	WT	Yes	heterozygous mutation 465 R→H
BE13	homozygous mutation 1601 L→P	WT	Yes	homozygous deletion
DU528	WT	WT	Yes	heterozygous mutation 465 R→H
HSB2	WT	WT	Yes	heterozygous mutation 505 R→C
Jurkat	WT	WT	Yes	heterozygous mutation 505 R→C
PF382	heterozygous mutation 1575 L→P	heterozygous insertion 2494 ASCILWTTPPATSYRCLSTPSSPRP LSPLTSGPSRPRIPTSPTGPRASPALPPACSPRSPAFRRPSSKRRAPRDP GFLSQAFGRLCALCGCQGRPEEPF*STOP	Yes	WT
Molt13	heterozygous mutation 1601 L→P	heterozygous deletion 2515 *STOP	Yes	WT
Supt7	heterozygous insertion 1593 F→LGA	heterozygous insertion 2429 AHKTYRCSSRTCSQQTSSSSKACSRHHHHHSR TLA*STOP	Yes	WT
Molt4	heterozygous mutation 1601 L→P	heterozygous deletion 2515 RVP*stop	Yes	WT
PEER	WT	WT	Yes	heterozygous mutation 505 R→C
Loucy	WT	WT	No	WT
Supt11	WT	WT	No	WT
Supt13	WT	WT	No	WT
Molt16	WT	WT	No	WT

[a]Numbers correspond to amino acid residues in NOTCH1.
[b]As determined by western blot analysis.

this ubiquitin ligase gene might account for the accumulation of NICD in T-ALL cell lines that lacked truncations of the NOTCH1 PEST degradation domain. Sequencing of the entire coding region of *FBW7* in 20 T-ALL cell lines revealed mutations in 6 of the 20 lines (30%) (Table I). The GSI-resistant cell line RPMI8402 harbored a homozygous arginine-to-histidine mutation at residue 465; all of the other mutations were heterozygous missense mutations of critical WD40 arginine residues (465 and 505). One additional cell line (BE13) has a homozygous deletion of *FBW7* as determined by quantitative DNA PCR. Each of the seven cell lines with increased levels of NICD but without C-terminal truncating mutations in *NOTCH1* (RPMI8402, CEM, BE13, DU528, HSB2, Jurkat, and PEER) harbored either a mutation in *FBW7* or homozygous deletion of the gene, thus providing an explanation for persistent NICD expression in these lines (Fig. 1 E). Conversely, none of the cell lines with *FBW7* mutations had PEST domain mutations in *NOTCH1*, suggesting that there is no selective pressure for *FBW7* mutation in cells with stabilized NOTCH1.

We also sequenced exons encoding the substrate-binding domain (exons 7, 8, 9, 10, and 11) of *FBW7* in 150 primary

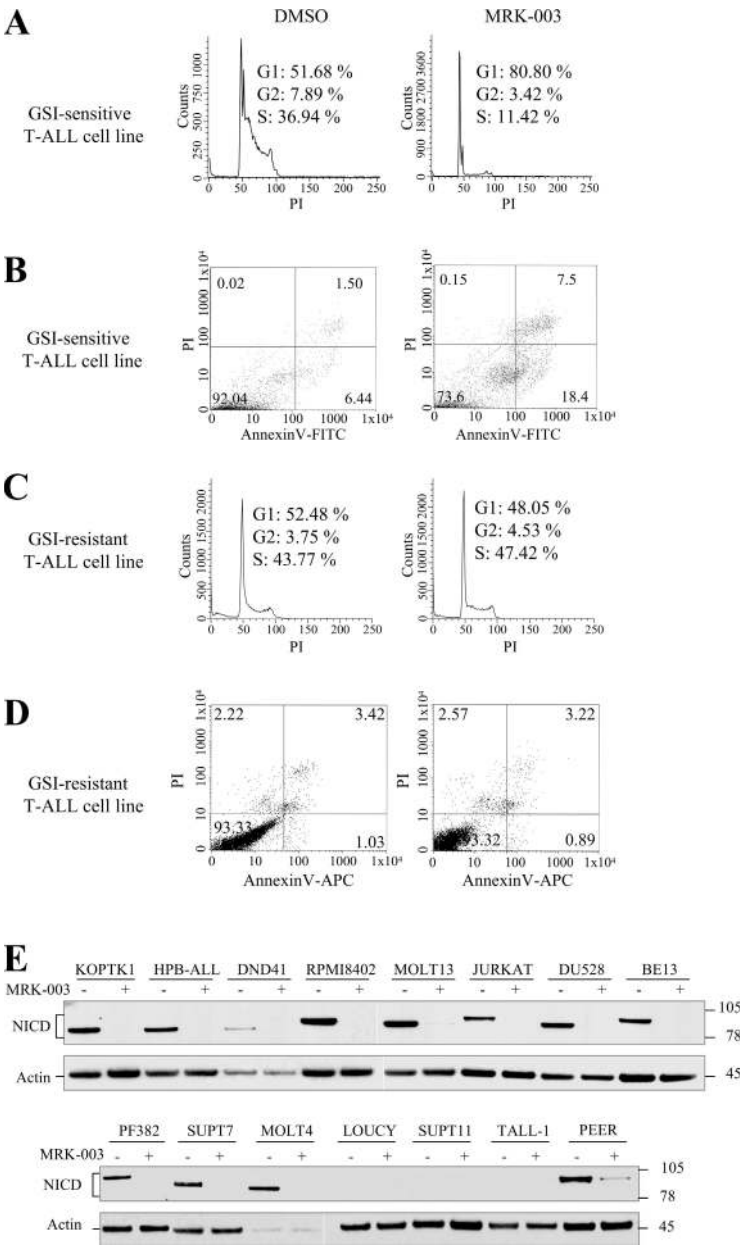

Figure 1. Treatment with MRK-003 results in cell cycle arrest, apoptosis, and inhibition of NICD production in human T-ALL cell lines. (A) Cell cycle analysis of the GSI-sensitive HPB-ALL cell line. Cells were treated with DMSO (vehicle) or 1 μM MRK-003 for 7 d, stained with propidium iodide, and analyzed by flow cytometry. (B) Annexin V–FITC/propidium iodide staining of the DND41 cell line after 7 d in DMSO or 1 μM MRK-003. Numbers represent the percentage of cells in each quadrant. Similar results were observed in other GSI-sensitive cell lines. (C) Cell cycle analysis of the GSI-resistant Molt13 cell line after 7 d in DMSO (vehicle) or MRK-003. Similar results were observed for all other GSI-resistant cell lines listed in Table I. (D) Annexin V–APC/propidium iodide staining of the Molt4 cell line after 7 d in DMSO or 1 μM MRK-003. Similar results were observed in all other GSI-resistant cell lines. (E) Activated NOTCH1 Western blot analysis. T-ALL cell lines were treated with 1 μM MRK-003 for 3 d. Whole cell lysates were subjected to SDS-PAGE electrophoresis and immunoblotting with the NOTCH1 (V1744) antibody.

acute myeloid leukemia (AML) samples, 60 primary myelodysplastic syndrome (MDS) samples, and 81 primary T-ALL samples. Although the AML or MDS samples lacked mutations in *FBW7*, 7 of 81 (8.6%) of the T-ALL samples harbored mutations in the substrate-binding domain of FBW7. All of the mutations in the patient samples were heterozygous missense mutations that altered arginine residues critical for substrate binding (Table II). As in the T-ALL cell lines, none of the primary samples with an *FBW7* mutation had C-terminal truncating mutations in *NOTCH1*. These results indicate that mutation of *FBW7* in primary T-ALL may represent an alternative mechanism of NOTCH deregulation that contributes to the pathogenesis this disease.

Table II. *FBW7* mutations in primary T-ALL patient samples

Sample[a]	*NOTCH1* status[b]		*FBW7* status
	HD domain	PEST domain	
2773	heterozygous mutation 1605 V→E	WT	heterozygous mutation 479 R→Q
2788	heterozygous mutation 1601 L→P	WT	heterozygous mutation 465 R→H
1179	WT	WT	heterozygous mutation 465 R→C
2748	heterozygous mutation 1586 L→P	WT	heterozygous mutation 479 R→Q
368	heterozygous mutation 1748 F→S	WT	heterozygous mutation 465 R→H
037	heterozygous mutation 1601 L→P	WT	heterozygous mutation 465 R→C
452	heterozygous mutation 1748 F→S	WT	heterozygous mutation 465 R→H

[a]The substrate binding encoding exons of *FBW7* were sequenced in 81 primary T-ALL patient samples. Mutations were found in 7 out of 81 (8.6%) Samples with mutations are shown.
[b]Numbers correspond to amino acid residues in NOTCH1.

The NOTCH1 T2512 region comprises an FBW7 phosphodegron

As outlined above, loss of FBW7-mediated regulation of its substrates can result from mutation of *FBW7* itself or from mutation of the substrate. The PEST domain of NICD is known to regulate protein stability and is a hot spot for mutations in primary human and mouse T-ALLs (7, 11). Furthermore, FBW7 binding to NOTCH is dependent on an intact PEST domain (27), strongly suggesting that the NOTCH CPD lies within this region. Alignment of the human NOTCH1 PEST domain with other FBW7 substrates demonstrated a CPD consensus motif anchored around threonine 2512 (T2512) in human NOTCH1. This residue is highly conserved across species as well as across members of the NOTCH family (Fig. 2 A). Notably, T-ALL–associated *NOTCH1* PEST mutations identified in both human and mouse tumors occur upstream, or very nearby, this putative CPD, suggesting that these mutations may disrupt its function (7, 11).

To determine if the T2512 region contains a functional NOTCH CPD, we examined its role in binding interactions between the NICD and FBW7. For these studies, we used an expression plasmid encoding the mouse NICD, where T2487 corresponds to human T2512 (human numbering is used to refer to this CPD throughout this article). We first mutated T2512 to alanine (T2512A) and cotransfected 293 cells (Fig. 2 B) or K562 erythroleukemia cells (Fig. 2 C) with FBW7 and NICD. Because the interaction of FBW7 with its substrates leads to ubiquitination and degradation by the proteasome, we uncoupled substrate binding from turnover so that we could observe stable FBW7–substrate interactions. To disrupt this pathway, we expressed two previously described SCF mutants: (a) dominant-negative cullin-1 (dnCul1), which interacts with F-box proteins, but not ubiquitin-conjugating enzymes (42), and (b) a truncated version of FBW7 (termed Fb-WD), which encodes the WD40 substrate binding domains but lacks the N-terminal domains, including the F-box motif, and thus is unable to associate with cullin-1 and with the SCF (43). In both cases we found that the T2512A NICD mutant showed markedly decreased binding to FBW7 when compared with WT-NICD (Fig. 2, B and C). In contrast, mutation of another possible NOTCH1 CPD consensus motif anchored around threonine 2133 (38) did not affect FBW7 binding (unpublished data).

Because two putative CDK8 sites in the T2512 region have been previously implicated in NOTCH degradation by FBW7 (S2514 and S2517), we also tested the role of these residues in FBW7 binding (26). We found that FBW7 binding was disrupted by the S2514A mutation and that binding was restored when S2514 was replaced by a phosphomimetic residue (S2514E) (Fig. 2 D). Although these data are consistent with a role for S2514 phosphorylation in FBW7 binding, a negative charge in the +2 position (relative to the central threonine) is not a characteristic CPD feature. We thus mutated S2514 to proline, which conforms to the CPD consensus, and found that S2514P also restored FBW7 binding. Thus, although a negative charge is tolerated in the +2 position, it is not required for FBW7 binding. We also examined the binding of the NICD to each of the three FBW7 isoforms, which reside in distinct subcellular compartments (44). The results show that NICD binds to both FBW7α (nucleoplasmic) and FBW7γ (nucleolar), but not to FBW7β (cytoplasmic), supporting the idea that the NICD interacts with FBW7 in the nucleus (Fig. 2 E).

We next examined the role of T2512 in directing FBW7-mediated endogenous NICD ubiquitination and, in accord with our binding studies, found that the T2512A mutation markedly reduces NICD ubiquitination (Fig. 2 F). The extent to which this mutation inhibited ubiquitination was similar to that seen with a C-terminal PEST deletion, termed deltaCT, which is defective in ubiquitination by FBW7 (27). The small amount of residual ubiquitination could reflect either basal, T2512A-independent interactions of the NICD with FBW7, or could be due to alternative NICD ubiquitination pathways. Finally, we used metabolic labeling and pulse chase to compare the half-life of WT-NICD to the T2512A mutant in 293 cells. As predicted, the T2512A mutant shows a prolonged half-life, reflecting impaired degradation in vivo (Fig. 2 G). Collectively, these data indicate that the T2512 region comprises a functional CPD that directs binding interactions between NOTCH and FBW7.

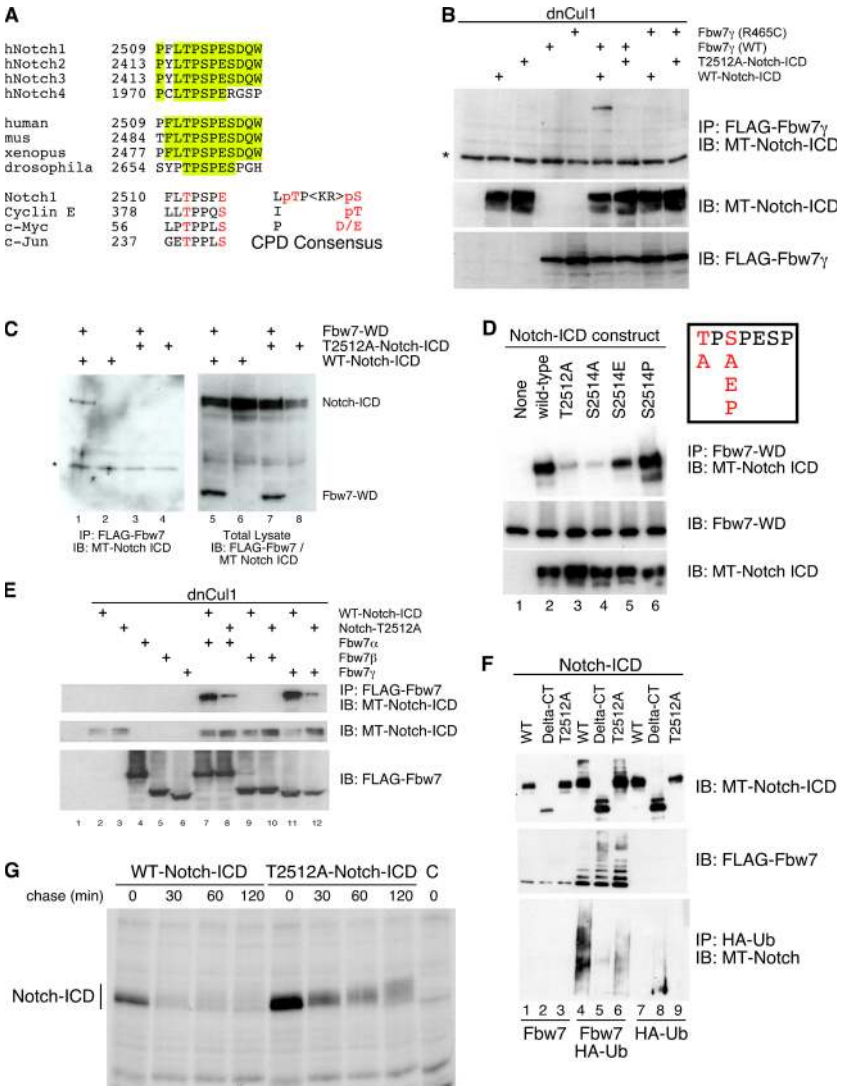

Figure 2. NOTCH T2512A mutant shows increased stability and decreased binding to FBW7. (A) Alignment of the four human NOTCH proteins, as well as Notch proteins from various species, shows strong conservation of the putative NOTCH CPD. Known CPDs are aligned with NOTCH for comparison. (B) The T2512A NOTCH mutant is deficient in binding to WT FBW7, and the tumor-derived FBW7 arginine mutant (R465C) can no longer bind WT NOTCH. Cells were transfected as indicated, and FLAG-FBW7 was immunoprecipitated. Samples were subjected to SDS-PAGE electrophoresis and immunoblotting with anti-MYC tag (9E10) to detect transfected Notch proteins. Whole cell lysates were analyzed as indicated to verify expression of transfected constructs. (C) Co-immunoprecipitation assays in the K562 erythroleukemia cell line show that T2512A is deficient in binding to FBW7 in hematopoietic cells. Whole cell lysates were analyzed as indicated to verify expression of transfected constructs. (D) Phosphorylation of S2514 is not required for the FBW7–Notch ICD interaction. 293a cells were transfected as indicated and analyzed as in B above. (E) NICD preferentially associates with nuclear and nucleolar FBW7 isoforms. 293a cells were transfected with the indicated plasmids and analyzed as in B above. (F) In vivo ubiquitination assays show that the NOTCH T2512A mutant is resistant to FBW7-mediated ubiquitination. 293a cells were transfected as indicated. Cell lysates were prepared and immunoprecipitated with anti-HA antibody to pull down ubiquitinated proteins. Samples were subjected to SDS-PAGE electrophoresis and immunoblotted with 9E10 to detect MYC-tagged NOTCH proteins. Whole cell lysates were analyzed as indicated to verify expression of transfected constructs. (G) The NOTCH T2512A mutant has an extended half-life in 293a cells compared with WT NOTCH. 293a cells were transfected with either WT NICD or the T2512A mutant. 48 h later, cells were pulse labeled in vivo with ^{35}S-methionine/cysteine and chased in medium with excess unlabeled methionine and cysteine for the indicated times. Transfected NOTCH proteins were immunoprecipitated with MN-1 antisera, and samples were subjected to SDS-PAGE electrophoresis. Gels were then exposed to x-ray film.

GSI treatment results in decreased MYC expression in a subset of T-ALL cell lines

Recent studies have demonstrated that *MYC* is a direct target of NOTCH in both human and mouse T-ALL (20–22). To determine if MYC protein levels are affected by treatment with MRK-003 in our panel of T-ALL cell lines, we performed Western blot analysis of lysates from a panel of 19 T-ALL cells that were either treated with vehicle

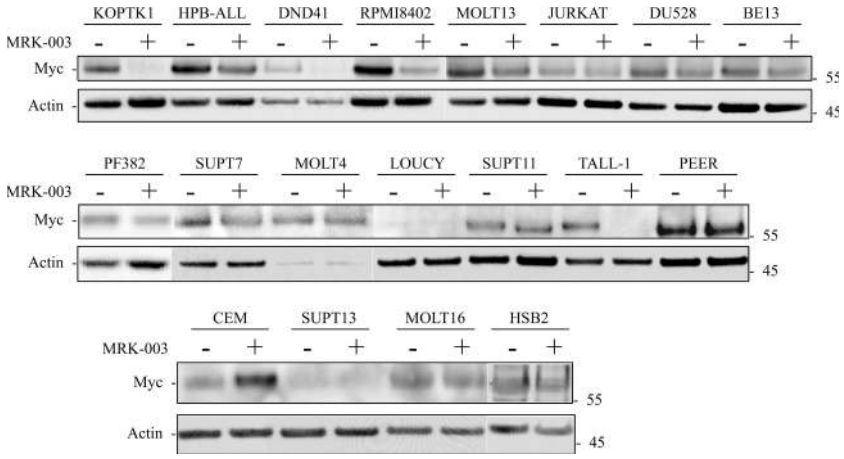

Figure 3. GSI treatment results in decreased MYC protein levels in a subset of T-ALL cell lines. T-ALL cell lines were treated with 1 μM MRK-003 or DMSO for 3 d, and whole cell lysates were prepared using RIPA lysis buffer. Western blot analysis was performed using antibodies against MYC and β-actin as a loading control.

(DMSO) or 1 μM MRK-003 for 3 d (Fig. 3). A reduction of MYC protein levels upon GSI treatment was apparent in 8 of the 19 lines (Koptk1, HPB-ALL, DND41, RPMI8402, Molt13, PF382, Supt7, and TALL1), including all of the GSI-sensitive lines tested (Koptk1, HPB-ALL, DND41, and TALL1). 4 of the other 10 lines (Loucy, Supt11, Supt13, and Molt16) lack activated NOTCH signaling (i.e., NICD was not detectable by Western blot analysis; Fig. 1 E and Table I), and thus we would not expect GSI treatment to affect the expression of NOTCH target genes in these lines. The remaining seven cell lines (Jurkat, Molt4, PEER, CEM, DU528, BE13, and HSB2) have activated NOTCH signaling but do not display decreased MYC expression upon GSI treatment. Of note, all of the cell lines in which MYC expression is not decreased upon GSI treatment are resistant to the drug, reinforcing the importance of this NOTCH target gene for T-ALL cell growth. Because overexpression of MYC has been shown to rescue the growth-suppressive effects of GSIs (20, 21), lack of MYC down-regulation in these T-ALL cell lines may contribute to their GSI resistance.

Because MYC is also a FBW7 target, we examined MYC half-life in a subset of five T-ALL cell lines (Molt4, DND41, KOPTK1, CEM, and Jurkat) by pulse-chase analysis. Although MYC half-life was prolonged in each cell line compared with a B cell lymphoblastoid cell line (JY) (Fig. 4), it was not increased in cell lines harboring mutations in *FBW7* (CEM and Jurkat) compared with those with WT *FBW7*. This result was not surprising because several lymphoblastic leukemia cell lines and patient samples have been shown to have aberrantly stabilized MYC (45). Thus, MYC may be stabilized in T-ALL cell lines without *FBW7* mutations due to mutations in other components of the MYC degradation pathway. Furthermore, in some contexts, FBW7 loss may lead to MYC stabilization in subcellular compartments (e.g., the nucleolus) without grossly altering bulk MYC turnover (44).

We also examined if *MYC* mRNA levels responded to GSI treatment by performing expression arrays on 18 of the T-ALL cell lines treated with DMSO or MRK-003 (1 μM) for 3 d. We observed either a very modest effect or no effect of GSI treatment on the levels of *MYC* RNA in four of the resistant lines that express NICD and have mutated *FBW7* (CEM, BE13, DU528, and HSB2) (Fig. 5). Hence, the lack of down-regulation of *MYC* by GSI treatment in these lines is due to mechanisms acting upstream of *MYC* transcription rather than at the protein level. In the microarray expression analysis, other NOTCH target genes such as *DELTEX1* and *SHQ1* (22) (Fig. 5 and not depicted) were also not affected by GSI treatment in the CEM, DU528, BE13, and HSB2 cell lines. In the PEER cell line, which also has a mutation in *FBW7*, we detected residual expression of NICD after 3 d of treatment with MRK-003, and quantitative RT-PCR showed that *MYC* and *DELTEX1* RNA expression levels did not decrease in this line upon GSI treatment (Fig. 1 E and not depicted). This suggests that the *FBW7* mutations (or homozygous deletion) found in these five lines result in residual signaling through NICD, even in the face of GSI treatment, thus sustaining *MYC* transcription and promoting continued cell proliferation.

Tumor-derived *FBW7* mutants are functionally impaired and may act as dominant-negative mutants to prevent MYC degradation

Because FBW7 is haploinsufficient for tumor suppression (46), the single allele *FBW7* mutations most commonly found in T-ALL could lead to stabilization of its substrates simply by reducing FBW7 activity by 50%. However, if the selective pressure for these mutations consisted simply of loss-of-function of one allele, we would predict that we would find nonsense mutations in the *FBW7* gene (36, 47). Our finding of mutational hot spots affecting the three key arginine residues of FBW7 argues against this possibility. Instead, we propose that

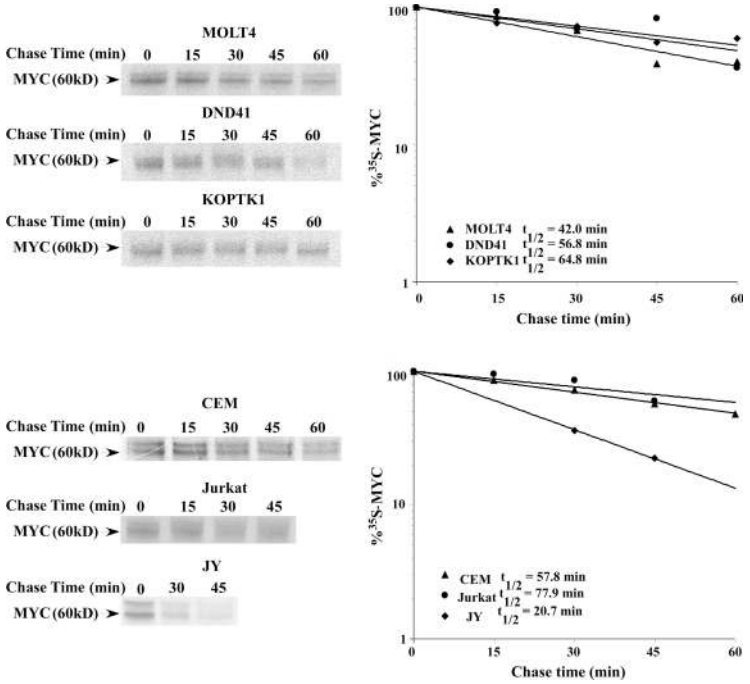

Figure 4. T-ALL cell lines have increased MYC half-life. (A) T-ALL cell lines with WT *FBW7* (Molt4, DND41 and KOPTK1) were pulse-labeled in vivo with ^{35}S-methionine/cysteine and chased in medium with excess unlabeled methionine and cysteine for the indicated times. Endogenous MYC was immunoprecipitated from an equal number of cells for each time point and analyzed by gel electrophoresis. ^{35}S-labeled MYC from each sample was quantitated by phosphoimager. The rate of degradation of MYC for each cell line is represented in the graph by best-fit exponential lines. Half-lives of MYC were calculated from exponential line equations. (B) Pulse-chase experiments were similarly performed on T-ALL cell lines with mutant *FBW7* (CEM and Jurkat). All T-ALL cell lines analyzed have increased MYC half-life compared with JY cells, a B cell lymphoblastoid cell line.

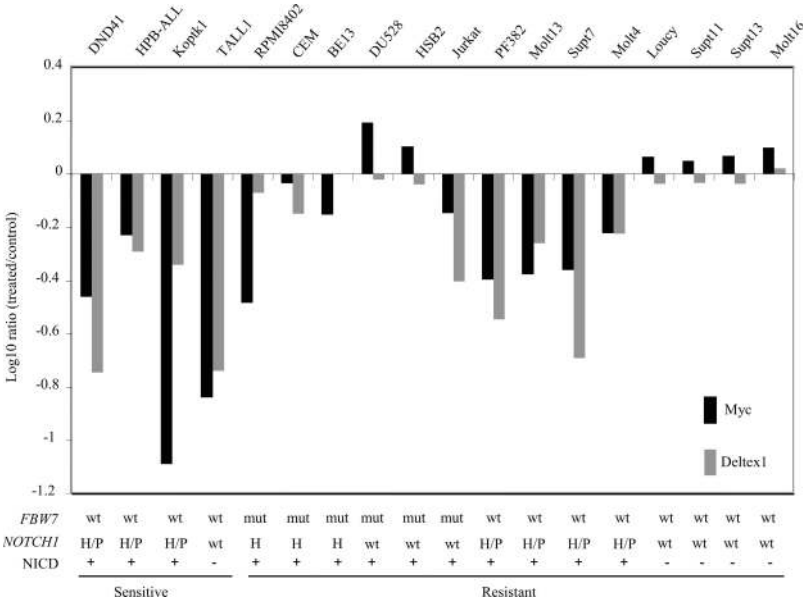

Figure 5. NOTCH target genes are not decreased upon GSI treatment in T-ALL cell lines with mutant *FBW7*. *MYC* and *DELTEX* RNA levels in 18 T-ALL cell lines after 3 d of 1 μM MRK-003 GSI treatment (compared with DMSO-treated cells) as determined by microarray gene expression analysis. Values are a $\log_{10}$ ratio of the expression level of *MYC* and *DELTEX* in MRK-003–treated cells compared with DMSO-treated cells.

the restricted mutational spectrum indicates a strong selection for expression of an FBW7 protein that is defective for productive substrate interactions and/or turnover, which suggests activity as a dominant-negative allele.

To explore this possibility, we analyzed each of the three mutant FBW7 proteins identified in T-ALL (Tables I and II) for their ability to bind to both MYC and NOTCH. As expected, the mutants were defective in NOTCH binding, although FBW7R479Q showed a modest amount of residual binding (Fig. 6 A, right). In contrast, each of the mutant FBW7 proteins bound to MYC, consistent with our recent finding that in addition to its canonical interaction with the MYC threonine 58 (T58) CPD, full-length FBW7 also binds to MYC through a second interaction that is independent of the T58 CPD (Fig. 6 A, left, and unpublished data). Importantly, although these FBW7 mutants bound to MYC, they were unable to promote MYC degradation (Fig. 6 B). We also examined whether a T-ALL–derived FBW7 mutant can dominantly interfere with FBW7-driven MYC degradation by expressing either increasing amounts of FBW7-γ or a mixture of a fixed amount of FBW7-γ in combination with increasing amounts of FBW7-γ-R465C. This analysis suggests that the mutant impairs FBW7-driven MYC degradation in a dose-dependent manner (Fig. 6 C).

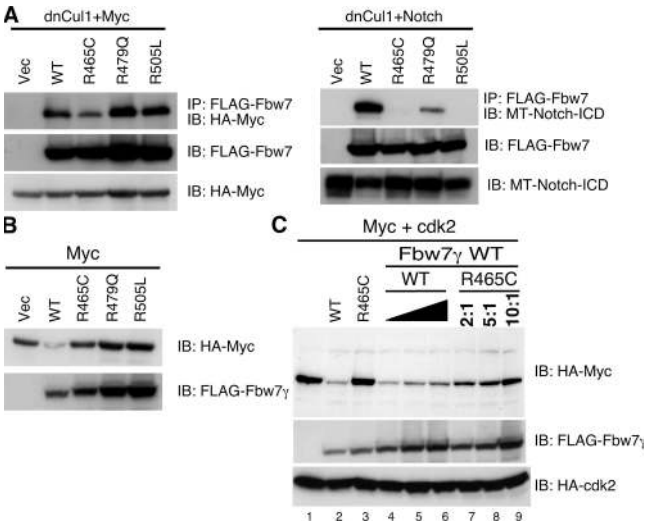

Figure 6. Mutant *FBW7* cannot bind to NICD and acts in a dominant-negative manner to prevent MYC degradation. (A) FBW7 arginine point mutants efficiently co-precipitate with MYC but not with NOTCH. 293a cells were transfected with the indicated plasmids. Whole cell lysates were subjected to immunoprecipitation with anti-FLAG, and resulting samples were analyzed via immunoblotting for either MT-NOTCH or HA-MYC as indicated. Whole cell lysates were also analyzed directly by SDS-PAGE and immunoblotting for FLAG-FBW7, HA-MYC, or MT-NOTCH as indicated to verify expression of transfected constructs. dnCul1 was included in all transfections to block FBW7-mediated proteasomal degradation. (B) T-ALL–associated FBW7 mutants are unable to mediate MYC degradation. 293a cells were transfected as indicated. Whole cell lysates were subjected to SDS-PAGE and immunoblotting for either HA-MYC or FLAG-FBW7 as indicated. (C) Tumor-derived FBW7 mutants dominantly inhibit MYC turnover by WT-FBW7. 293a cells were transfected with a constant amount of HA-MYC with increasing amounts of either FLAG-FBW7-γ or a combination of a constant amount (500 ng) of FLAG-FBW7-γ and increasing amounts of FLAG-FBW7-γ-R465H (1–5 μg). The ratios of mutant to WT FBW7 expression are indicated above lanes 7–9. HA-cdk2, which does not affect turnover of MYC by FBW7, is included as a transfection control. Whole cell lysates were subjected to SDS-PAGE and immunoblotting for HA-MYC, HA-cdk2, or FLAG-FBW7 as indicated.

At least two mechanisms may contribute to the dominant-negative activities of the mutant FBW7 proteins. The first is suggested by our finding that the FBW7 mutants still interact with Myc through a binding interaction independent of the MYC CPD that cannot promote MYC degradation. Hence, in the case of MYC, they may simply compete with WT FBW7 for MYC binding. However, a second mechanism of dominant-negative function is suggested by recent findings that FBW7 (and its orthologs) form dimers (48–51), thus raising the possibility that WT and mutant FBW7 proteins form heterodimeric dominant-negative complexes that are unable to degrade MYC. However, because mutation of the FBW7 dimerization region also disrupts its noncanonical binding interaction with MYC, we cannot currently distinguish between these two possibilities (unpublished data). We thus propose that *FBW7* mutations may contribute to T-ALL pathogenesis and GSI resistance by leading to the stabilization of MYC as well as NICD.

DISCUSSION

The early successes of molecularly targeted therapy, such as imatinib mesylate directed against the BCR-ABL fusion protein in chronic myelogenous leukemia, stimulated enormous interest in subverting abnormal signaling pathways in cancer cells. The NOTCH signaling cascade influences normal development by regulating differentiation, proliferation, and apoptosis (52). Activation of the NOTCH signaling pathway is firmly established in T-ALL and is likely involved in the genesis of many other tumor types (53). Thus, it is not surprising that efforts to block NOTCH signaling as a novel therapeutic strategy are under way in T-ALL as well as in solid tumors. One of the most promising approaches has been to inhibit NOTCH receptor signaling using GSIs. This strategy suppresses the generation of NICD and thus, in principle, should inhibit the downstream transcriptional events normally induced by this key signaling component after it traverses to the nucleus. Although effective against some T-ALL cell lines, GSIs do not uniformly eliminate leukemic cells with activated NOTCH signaling. Understanding the mechanisms of GSI resistance may lead to better treatments for T-ALL.

We found missense *FBW7* mutations or homozygous *FBW7* deletion in GSI-resistant T-ALL cell lines and in primary T-ALL samples. Moreover, we have defined the NOTCH phosphodegron and demonstrated that the mutant forms of FBW7 found in T-ALL cannot bind to the NICD. Each T-ALL cell line with constitutive NICD expression harbored either *NOTCH1* PEST domain or *FBW7* mutations, suggesting that these two classes of mutations provide a mutually exclusive

means of prolonging the NICD half-life. We also show that the expression of NOTCH target genes including *DELTEX1* and *MYC* are not affected by GSI treatment in five resistant T-ALL cell lines with mutations in *FBW7* (CEM, BE13, PEER, DU528, and HSB2), demonstrating that the mechanism of resistance in these leukemias lies upstream of *MYC* and *DELTEX1* transcription. It appears that in these T-ALL lines, one consequence of *FBW7* mutation is stabilization of the NICD resulting in sustained NOTCH signaling, and thus promoting resistance to GSIs. However, other FBW7 substrates, such as MYC, may also account for selection for *FBW7* mutations and for GSI resistance in T-ALL, as suggested by our finding that ALL-associated *FBW7* mutations can dominantly inhibit MYC degradation.

An important question is why *FBW7* mutation confers GSI resistance, whereas NOTCH PEST domain truncations that remove the FBW7 interaction domain do not. In each cell line with PEST mutations, only one allele is affected by these heterozygous mutations, leaving the remaining normal allele, which encodes an NICD that is stabilized in the presence of mutant FBW7. Thus, although the amount of increased NOTCH activity resulting from the single allele PEST mutations may be sufficient to underlie the primary selection for these mutations, disruption of FBW7 function may be more active in sustaining NOTCH signaling and also may prolong the half-life of MYC (as well as other substrates), thus promoting GSI drug resistance.

The association between *FBW7* mutations and resistance to GSIs has implications for clinical testing of these agents in patients whose cancers show deregulation of the NOTCH pathway. Molecular analysis of the *FBW7* gene, as well as genes encoding the relevant NOTCH receptors and other key components of the NOTCH signaling pathway, such as NUMB, may contribute to identification of patients likely to be most responsive to GSI therapy. Because Myc has recently been shown to be an important target of Notch in mammary tumorigenesis as well as in T-ALL (5), it might also be possible to overcome GSI resistance by combining GSIs with other drugs that block the MYC pathway to synergistically reduce MYC levels and block tumor cell growth. One attractive candidate is TMPyP4, a cationic porphyrin that binds to and stabilizes guanine quadruplexes in DNA. *MYC* contains a sequence in its promoter that forms a guanine quadruplex, and TMPyP4 has been shown to inhibit *MYC* transcription and the growth of tumor cells in vivo (54). Thus, TMPyP4 or other agents that inhibit *MYC* transcription may be useful in combination with GSIs to overcome resistance in patients harboring *FBW7* mutations. Pharmacologic or genetic strategies that restore the normal function of FBW7 in tumor cells could also be therapeutically useful.

MATERIALS AND METHODS

Patient samples. Bone marrow or peripheral blood samples were collected at diagnosis from T-ALL patients at the Sophia Children's Hospital/Erasmus MC and the Dutch Childhood Oncology Group, as well as from AML, MDS, and T-ALL patients at Dana-Farber Cancer Institute. Informed consent and Institutional Review Board approval was obtained to use leftover patient material for research purposes.

Cell lines. T-ALL cell lines were obtained from American Type Culture Collection or Deutsche Sammlung von Mikroorganismen und Zellkulturen GmbH. 293a cells were provided by S. Reed (The Scripps Research Institute, La Jolla, CA).

Treatment of T-ALL cell lines with MRK-003. T-ALL cell lines were plated at a density of 5×10^4–1.5×10^5 cells per ml (depending on doubling time) and were treated with either DMSO or 1 μM MRK-003 for 0 h, 6 h, 24 h, 3 d, or 7 d. For each time point, triplicate flasks were analyzed by the trypan blue exclusion assay to determine cell viability. For propidium iodide staining to analyze the cell cycle profile, cells were washed with PBS, stained in a PBS buffer containing 50 μg/ml propidium iodide and 200 μg/ml RNase A, and analyzed on a Becton Dickinson FACSCalibur Instrument. For annexin V staining to determine the percentage of cells undergoing apoptosis, the annexin V–FITC (or annexin V–APC) Apoptosis detection kit I (BD Biosciences) was used according to the manufacturer's instructions.

Microarray gene expression analysis. Total RNA isolated from cultured cells was used to make fluorescently labeled cRNA that was hybridized to DNA oligonucleotide microarrays as described previously (55, 56). Human microarrays contained oligonucleotide probes corresponding to ~21,000 genes. All oligonucleotide probes on the microarrays were synthesized in situ with inkjet technology (Agilent Technologies) (55). After hybridization, arrays were scanned and fluorescence intensities for each probe were recorded. Ratios of transcript abundance (experimental to control) were obtained after normalization and correction of the array intensity data. Gene expression data were analyzed with the Rosetta Resolver gene expression analysis software (version 6.0; Rosetta Biosoftware). Microarray data have been deposited in the GEO database under accession number GSE8416.

Western blotting. For analysis of endogenous protein expression, T-ALL cell lines were treated with MRK-003 for 3 d and lysed in RIPA buffer. Blots were probed with 9E10 anti-MYC antibody (1:500; Santa Cruz Biotechnology, Inc.), the cleaved NOTCH1 (Val1744) antibody (1:1,000; Cell Signaling Technology) as described previously (24), and anti–β-actin (1:7,000; Abcam) for the loading control. Signal was detected with Super-Signal West Femto ECL reagent (Pierce Chemical Co.). For transfections, MYC-tagged proteins were detected with 9E10 hybridoma supernatant (1:4), HA-tagged proteins were detected with HA-11 (1:1,000), and FLAG-tagged proteins were detected with M2 anti-FLAG (1:4,000; Sigma-Aldrich). These same antibodies were conjugated to protein G sepharose and used for immunoprecipitations as described previously (57).

Mutation detection. The entire coding region of *FBW7* was sequenced in genomic DNA isolated from the 20 T-ALL cell lines. Exons 7, 8, 9, 10, and 11 of *FBW7* were sequenced in primary patient samples. All sequencing was performed at Agencourt Bioscience Corporation. Residues are numbered according to their location in the α isoform of FBW7 (GenBank RefSeq NM_033632).

Plasmids and transient transfections. The following expression plasmids have been described (43, 44): pFLAG-FBW7-α, -β, and -γ; pFLAG-FbWD; pFLAG-FBW7-γ-R465H (also termed R298H); and HA-MYC, HA-dncul1, and HA-ubiquitin. All mutagenesis were performed by the QuickChange method (Stratagene) and confirmed by sequencing. Point mutations in the FBW7 common region R465H, R479Q, and R505C were generated by site-directed mutagenesis using pFLAG-FBW7 vectors as template. Although numbering is different between isoforms, the α numbering is used for simplicity. CS2-mNICD-MT was provided by R. Kopan (Washington University, St. Louis, MO). It encodes the mouse Notch1 intracellular domain from Val1744 to the end of the WT protein and includes six in-frame MYC epitope

tags at the C terminus. Mutagenesis of this construct was used to generate the T2512A, S2514A, S2514E, and S2514P mutants. The deltaCT mutation, generated by PCR, deletes the PEST domain but maintains the C-terminal MYC tags. 293A cells were transfected by the calcium phosphate precipitation method as described previously (57). Cells were harvested at 36–48 h after transfection using TENT buffer (50 MM Tris-Cl, pH 8.0, 2 mM EDTA, 150 mM NaCl, 1% Triton X-100) (30) with protease and phosphatase inhibitors and analyzed by immunoprecipitation and Western blotting as described previously (57).

Metabolic labeling and pulse chase. NICD pulse-chase assays were performed as described previously (43). In brief, 293a cells were transfected with plasmids encoding MYC-tagged NICD or NICD T2512A. At 36 h after transfection, cells were preincubated with media lacking cysteine and methionine, pulsed with media containing Trans 35S label, and chased with media with cold methionine. Samples were obtained at the indicated time points and immunoprecipitated with anti-Notch serum MN1, a mouse monoclonal antibody recognizing the NICD (provided by I. Bernstein, Fred Hutchinson Cancer Research Center, Seattle, WA). MYC pulse-chase experiments were performed as described previously (45).

Ubiquitination assays. Cell-based ubiquitination assays were performed as described previously (58). In brief, transiently transfected 293a cells were harvested at 48 h after transfection. Cells were trypsinized, rinsed once with PBS, and lysed in 100 μl 2% SDS in TBS (10 mM Tris-HCl, pH 8.0, 150 mM NaCl) with boiling for 10 min. These samples were diluted at 1:10 with 1% triton in TBS containing protease inhibitors, 5 mM N-ethymaleimide, and 5 mM MG132, sonicated, precleared with protein G sepharose, and centrifuged to pellet-insoluble debris. Aliquots were removed for Western blot analysis, and the remaining lysates were immunoprecipitated with anti-HA antisera prebound to protein G sepharose. Samples were analyzed by SDS-PAGE and probed with 9E10 to visualize MYC-tagged ubiquitinated Notch proteins.

The authors wish to thank Theresa Zhang, Leslie Carlini, and Xudong Dai for helpful discussions regarding mRNA profiling; Hellen Kim for discussions about Western blotting methods; Keith McKenna and Chitra Raghunathan for technical assistance; and John Gilbert for editorial review.

This work was funded by a sponsored research agreement from Merck Research Laboratories (to A.T. Look), an American Society of Hematology Fellow Scholar Award and by the National Institutes of Health (1K08CA109124-01A2; to J. Grim), National Institutes of Health grants (R01CA84069 and R01CA102742) and the Burroughs Welcome Foundation (to B.E. Clurman), as well as a Harvard Medical School Hematology Training Grant (to J. O'Neil).

The authors have no conflicting financial interests.

Submitted: 2 May 2007
Accepted: 28 June 2007

REFERENCES

1. Wilson, A., and F. Radtke. 2006. Multiple functions of Notch signaling in self-renewing organs and cancer. *FEBS Lett.* 580:2860–2868.
2. Gallahan, D., and R. Callahan. 1987. Mammary tumorigenesis in feral mice: identification of a new int locus in mouse mammary tumor virus (Czech II)-induced mammary tumors. *J. Virol.* 61:66–74.
3. Dievart, A., N. Beaulieu, and P. Jolicoeur. 1999. Involvement of Notch1 in the development of mouse mammary tumors. *Oncogene.* 18:5973–5981.
4. Hallahan, A.R., J.I. Pritchard, S. Hansen, M. Benson, J. Stoeck, B.A. Hatton, T.L. Russell, R.G. Ellenbogen, I.D. Bernstein, P.A. Beachy, and J.M. Olson. 2004. The SmoA1 mouse model reveals that notch signaling is critical for the growth and survival of sonic hedgehog-induced medulloblastomas. *Cancer Res.* 64:7794–7800.
5. Klinakis, A., M. Szabolcs, K. Politi, H. Kiaris, S. Artavanis-Tsakonas, and A. Efstratiadis. 2006. Myc is a Notch1 transcriptional target and a requisite for Notch1-induced mammary tumorigenesis in mice. *Proc. Natl. Acad. Sci. USA.* 103:9262–9267.
6. Pear, W.S., J.C. Aster, M.L. Scott, R.P. Hasserjian, B. Soffer, J. Sklar, and D. Baltimore. 1996. Exclusive development of T cell neoplasms in mice transplanted with bone marrow expressing activated Notch alleles. *J. Exp. Med.* 183:2283–2291.
7. O'Neil, J., J. Calvo, K. McKenna, V. Krishnamoorthy, J.C. Aster, C.H. Bassing, F.W. Alt, M. Kelliher, and A.T. Look. 2006. Activating Notch1 mutations in mouse models of T-ALL. *Blood.* 107:781–785.
8. Mantha, S., M. Ward, J. McCafferty, A. Herron, T. Palomero, A. Ferrando, A. Bank, and C. Richardson. 2007. Activating Notch1 mutations are an early event in T-cell malignancy of Ikaros point mutant Plastic/+ mice. *Leuk. Res.* 31:321–327.
9. Lin, Y.W., R.A. Nichols, J.J. Letterio, and P.D. Aplan. 2006. Notch1 mutations are important for leukemic transformation in murine models of precursor-T leukemia/lymphoma. *Blood.* 107:2540–2543.
10. Ellisen, L.W., J. Bird, D.C. West, A.L. Soreng, T.C. Reynolds, S.D. Smith, and J. Sklar. 1991. TAN-1, the human homolog of the Drosophila notch gene, is broken by chromosomal translocations in T lymphoblastic neoplasms. *Cell.* 66:649–661.
11. Weng, A.P., A.A. Ferrando, W. Lee, J.P. Morris, L.B. Silverman, C. Sanchez-Irizarry, S.C. Blacklow, A.T. Look, and J.C. Aster. 2004. Activating mutations of NOTCH1 in human T cell acute lymphoblastic leukemia. *Science.* 306:269–271.
12. Park, J.T., M. Li, K. Nakayama, T.L. Mao, B. Davidson, Z. Zhang, R.J. Kurman, C.G. Eberhart, M. Shih Ie, and T.L. Wang. 2006. Notch3 gene amplification in ovarian cancer. *Cancer Res.* 66:6312–6318.
13. Pece, S., M. Serresi, E. Santolini, M. Capra, E. Hulleman, V. Galimberti, S. Zurrida, P. Maisonneuve, G. Viale, and P.P. Di Fiore. 2004. Loss of negative regulation by Numb over Notch is relevant to human breast carcinogenesis. *J. Cell Biol.* 167:215–221.
14. Jundt, F., I. Anagnostopoulos, R. Forster, S. Mathas, H. Stein, and B. Dorken. 2002. Activated Notch1 signaling promotes tumor cell proliferation and survival in Hodgkin and anaplastic large cell lymphoma. *Blood.* 99:3398–3403.
15. Balint, K., M. Xiao, C.C. Pinnix, A. Soma, I. Veres, I. Juhasz, E.J. Brown, A.J. Capobianco, M. Herlyn, and Z.J. Liu. 2005. Activation of Notch1 signaling is required for beta-catenin-mediated human primary melanoma progression. *J. Clin. Invest.* 115:3166–3176.
16. Purow, B.W., R.M. Haque, M.W. Noel, Q. Su, M.J. Burdick, J. Lee, T. Sundaresan, S. Pastorino, J.K. Park, I. Mikolaenko, et al. 2005. Expression of Notch-1 and its ligands, Delta-like-1 and Jagged-1, is critical for glioma cell survival and proliferation. *Cancer Res.* 65:2353–2363.
17. Haruki, N., K.S. Kawaguchi, S. Eichenberger, P.P. Massion, S. Olson, A. Gonzalez, D.P. Carbone, and T.P. Dang. 2005. Dominant-negative Notch3 receptor inhibits mitogen-activated protein kinase pathway and the growth of human lung cancers. *Cancer Res.* 65:3555–3561.
18. Collins, B.J., W. Kleeberger, and D.W. Ball. 2004. Notch in lung development and lung cancer. *Semin. Cancer Biol.* 14:357–364.
19. Santagata, S., F. Demichelis, A. Riva, S. Varambally, M.D. Hofer, J.L. Kutok, R. Kim, J. Tang, J.E. Montie, A.M. Chinnaiyan, et al. 2004. JAGGED1 expression is associated with prostate cancer metastasis and recurrence. *Cancer Res.* 64:6854–6857.
20. Weng, A.P., J.M. Millholland, Y. Yashiro-Ohtani, M.L. Arcangeli, A. Lau, C. Wai, C. Del Bianco, C.G. Rodriguez, H. Sai, J. Tobias, et al. 2006. c-Myc is an important direct target of Notch1 in T-cell acute lymphoblastic leukemia/lymphoma. *Genes Dev.* 20:2096–2109.
21. Sharma, V.M., J.A. Calvo, K.M. Draheim, L.A. Cunningham, N. Hermance, L. Beverly, V. Krishnamoorthy, M. Bhasin, A.J. Capobianco, and M.A. Kelliher. 2006. Notch1 contributes to mouse T-cell leukemia by directly inducing the expression of c-myc. *Mol. Cell. Biol.* 26:8022–8031.
22. Palomero, T., W.K. Lim, D.T. Odom, M.L. Sulis, P.J. Real, A. Margolin, K.C. Barnes, J. O'Neil, D. Neuberg, A.P. Weng, et al. 2006. NOTCH1 directly regulates c-MYC and activates a feed-forward-loop transcriptional network promoting leukemic cell growth. *Proc. Natl. Acad. Sci. USA.* 103:18261–18266.
23. Jarriault, S., C. Brou, F. Logeat, E.H. Schroeter, R. Kopan, and A. Israel. 1995. Signalling downstream of activated mammalian Notch. *Nature.* 377:355–358.
24. Lewis, H., M. Leveridge, P.R. Strack, C.D. Haldon, J. O'Neil, H. Kim, A. Madin, C. Joanne, J.C. Hannam, A.T. Look, et al. 2007. Apoptosis in

T-cell acute lymphoblastic leukemia cells following cell-cycle arrest induced by pharmacological inhibition of Notch signaling. *Chem. Biol.* 14:209–219.
25. Tetzlaff, M.T., W. Yu, M. Li, P. Zhang, M. Finegold, K. Mahon, J.W. Harper, R.J. Schwartz, and S.J. Elledge. 2004. Defective cardiovascular development and elevated cyclin E and Notch proteins in mice lacking the Fbw7 F-box protein. *Proc. Natl. Acad. Sci. USA.* 101:3338–3345.
26. Fryer, C.J., J.B. White, and K.A. Jones. 2004. Mastermind recruits CycC:CDK8 to phosphorylate the Notch ICD and coordinate activation with turnover. *Mol. Cell.* 16:509–520.
27. Oberg, C., J. Li, A. Pauley, E. Wolf, M. Gurney, and U. Lendahl. 2001. The Notch intracellular domain is ubiquitinated and negatively regulated by the mammalian Sel-10 homolog. *J. Biol. Chem.* 276:35847–35853.
28. Tsunematsu, R., K. Nakayama, Y. Oike, M. Nishiyama, N. Ishida, S. Hatakeyama, Y. Bessho, R. Kageyama, T. Suda, and K.I. Nakayama. 2004. Mouse Fbw7/Sel-10/Cdc4 is required for notch degradation during vascular development. *J. Biol. Chem.* 279:9417–9423.
29. Gupta-Rossi, N., O. Le Bail, H. Gonen, C. Brou, F. Logeat, E. Six, A. Ciechanover, and A. Israel. 2001. Functional interaction between SEL-10, an F-box protein, and the nuclear form of activated Notch1 receptor. *J. Biol. Chem.* 276:34371–34378.
30. Wu, G., S. Lyapina, I. Das, J. Li, M. Gurney, A. Pauley, I. Chui, R.J. Deshaies, and J. Kitajewski. 2001. SEL-10 is an inhibitor of notch signaling that targets notch for ubiquitin-mediated protein degradation. *Mol. Cell. Biol.* 21:7403–7415.
31. Minella, A.C., and B.E. Clurman. 2005. Mechanisms of tumor suppression by the SCF(Fbw7). *Cell Cycle.* 4:1356–1359.
32. Orlicky, S., X. Tang, A. Willems, M. Tyers, and F. Sicheri. 2003. Structural basis for phosphodependent substrate selection and orientation by the SCFCdc4 ubiquitin ligase. *Cell.* 112:243–256.
33. Nash, P., X. Tang, S. Orlicky, Q. Chen, F.B. Gertler, M.D. Mendenhall, F. Sicheri, T. Pawson, and M. Tyers. 2001. Multisite phosphorylation of a CDK inhibitor sets a threshold for the onset of DNA replication. *Nature.* 414:514–521.
34. Yada, M., S. Hatakeyama, T. Kamura, M. Nishiyama, R. Tsunematsu, H. Imaki, N. Ishida, F. Okumura, K. Nakayama, and K.I. Nakayama. 2004. Phosphorylation-dependent degradation of c-Myc is mediated by the F-box protein Fbw7. *EMBO J.* 23:2116–2125.
35. Kwak, E.L., K.H. Moberg, D.C. Wahrer, J.E. Quinn, P.M. Gilmore, C.A. Graham, I.K. Hariharan, D.P. Harkin, D.A. Haber, and D.W. Bell. 2005. Infrequent mutations of Archipelago (hAGO, hCDC4, Fbw7) in primary ovarian cancer. *Gynecol. Oncol.* 98:124–128.
36. Kemp, Z., A. Rowan, W. Chambers, N. Wortham, S. Halford, O. Sieber, N. Mortensen, A. von Herbay, T. Gunther, M. Ilyas, and I. Tomlinson. 2005. CDC4 mutations occur in a subset of colorectal cancers but are not predicted to cause loss of function and are not associated with chromosomal instability. *Cancer Res.* 65:11361–11366.
37. Spruck, C.H., H. Strohmaier, O. Sangfelt, H.M. Muller, M. Hubalek, E. Muller-Holzner, C. Marth, M. Widschwendter, and S.I. Reed. 2002. hCDC4 gene mutations in endometrial cancer. *Cancer Res.* 62: 4535–4539.
38. Wei, W., J. Jin, S. Schlisio, J.W. Harper, and W.G. Kaelin Jr. 2005. The v-Jun point mutation allows c-Jun to escape GSK3-dependent recognition and destruction by the Fbw7 ubiquitin ligase. *Cancer Cell.* 8:25–33.
39. Bhatia, K., G. Spangler, G. Gaidano, N. Hamdy, R. Dalla-Favera, and I. Magrath. 1994. Mutations in the coding region of c-myc occur frequently in acquired immunodeficiency syndrome-associated lymphomas. *Blood.* 84:883–888.
40. Yano, T., C.A. Sander, H.M. Clark, M.V. Dolezal, E.S. Jaffe, and M. Raffeld. 1993. Clustered mutations in the second exon of the MYC gene in sporadic Burkitt's lymphoma. *Oncogene.* 8:2741–2748.
41. Bhatia, K., K. Huppi, G. Spangler, D. Siwarski, R. Iyer, and I. Magrath. 1993. Point mutations in the c-Myc transactivation domain are common in Burkitt's lymphoma and mouse plasmacytomas. *Nat. Genet.* 5:56–61.
42. Ye, X., G. Nalepa, M. Welcker, B.M. Kessler, E. Spooner, J. Qin, S.J. Elledge, B.E. Clurman, and J.W. Harper. 2004. Recognition of phosphodegron motifs in human cyclin E by the SCF(Fbw7) ubiquitin ligase. *J. Biol. Chem.* 279:50110–50119.
43. Welcker, M., A. Orian, J. Jin, J.E. Grim, J.W. Harper, R.N. Eisenman, and B.E. Clurman. 2004. The Fbw7 tumor suppressor regulates glycogen synthase kinase 3 phosphorylation-dependent c-Myc protein degradation. *Proc. Natl. Acad. Sci. USA.* 101:9085–9090.
44. Welcker, M., A. Orian, J.E. Grim, R.N. Eisenman, and B.E. Clurman. 2004. A nucleolar isoform of the Fbw7 ubiquitin ligase regulates c-Myc and cell size. *Curr. Biol.* 14:1852–1857.
45. Malempati, S., D. Tibbitts, M. Cunningham, Y. Akkari, S. Olson, G. Fan, and R.C. Sears. 2006. Aberrant stabilization of c-Myc protein in some lymphoblastic leukemias. *Leukemia.* 20:1572–1581.
46. Mao, J.H., J. Perez-Losada, D. Wu, R. Delrosario, R. Tsunematsu, K.I. Nakayama, K. Brown, S. Bryson, and A. Balmain. 2004. Fbxw7/Cdc4 is a p53-dependent, haploinsufficient tumour suppressor gene. *Nature.* 432:775–779.
47. Rajagopalan, H., P.V. Jallepalli, C. Rago, V.E. Velculescu, K.W. Kinzler, B. Vogelstein, and C. Lengauer. 2004. Inactivation of hCDC4 can cause chromosomal instability. *Nature.* 428:77–81.
48. Zhang, W., and D.M. Koepp. 2006. Fbw7 isoform interaction contributes to cyclin E proteolysis. *Mol. Cancer Res.* 4:935–943.
49. Welcker, M., and B.E. Clurman. 2007. Fbw7/hCDC4 dimerization regulates its substrate interactions. *Cell Div.* 2:7.
50. Hao, B., S. Oehlmann, M.E. Sowa, J.W. Harper, and N.P. Pavletich. 2007. Structure of a Fbw7-Skp1-cyclin E complex: multisite-phosphorylated substrate recognition by SCF ubiquitin ligases. *Mol. Cell.* 26:131–143.
51. Tang, X., S. Orlicky, Z. Lin, A. Willems, D. Neculai, D. Ceccarelli, F. Mercurio, B.H. Shilton, F. Sicheri, and M. Tyers. 2007. Suprafacial orientation of the SCF(Cdc4) dimer accommodates multiple geometries for substrate ubiquitination. *Cell.* 129:1165–1176.
52. Artavanis-Tsakonas, S., M.D. Rand, and R.J. Lake. 1999. Notch signaling: cell fate control and signal integration in development. *Science.* 284:770–776.
53. Miele, L., T. Golde, and B. Osborne. 2006. Notch signaling in cancer. *Curr. Mol. Med.* 6:905–918.
54. Grand, C.L., H. Han, R.M. Munoz, S. Weitman, D.D. Von Hoff, L.H. Hurley, and D.J. Bearss. 2002. The cationic porphyrin TMPyP4 down-regulates c-MYC and human telomerase reverse transcriptase expression and inhibits tumor growth in vivo. *Mol. Cancer Ther.* 1:565–573.
55. Hughes, T.R., M. Mao, A.R. Jones, J. Burchard, M.J. Marton, K.W. Shannon, S.M. Lefkowitz, M. Ziman, J.M. Schelter, M.R. Meyer, et al. 2001. Expression profiling using microarrays fabricated by an ink-jet oligonucleotide synthesizer. *Nat. Biotechnol.* 19:342–347.
56. Marton, M.J., J.L. DeRisi, H.A. Bennett, V.R. Iyer, M.R. Meyer, C.J. Roberts, R. Stoughton, J. Burchard, D. Slade, H. Dai, et al. 1998. Drug target validation and identification of secondary drug target effects using DNA microarrays. *Nat. Med.* 4:1293–1301.
57. Clurman, B.E., R.J. Sheaff, K. Thress, M. Groudine, and J.M. Roberts. 1996. Turnover of cyclin E by the ubiquitin-proteasome pathway is regulated by cdk2 binding and cyclin phosphorylation. *Genes Dev.* 10:1979–1990.
58. Buschmann, T., S.Y. Fuchs, C.G. Lee, Z.Q. Pan, and Z. Ronai. 2000. SUMO-1 modification of Mdm2 prevents its self-ubiquitination and increases Mdm2 ability to ubiquitinate p53. *Cell.* 101:753–762.